Data Article

# Dataset on *in-silico* investigation on triazole derivatives via molecular modelling approach: A potential glioblastoma inhibitors

Abel Kolawole Oyebamiji [a,g,*], Oluwatumininu Abosede Mutiu [b], Folake Ayobami Amao [c], Olubukola Monisola Oyawoye [d], Temitope A Oyedepo [e], Babatunde Benjamin Adeleke [f], Banjo Semire [g]

[a] *Department of Basic Sciences, Adeleke University, P.M.B. 250, Ede, Osun State, Nigeria*
[b] *Department of Chemical Sciences, Osun State University, Osogbo, Osun State, Nigeria*
[c] *Department of Mathematics, Faculty of Science, Adeleke University, P.M.B. 250, Ede, Osun State, Nigeria*
[d] *Department of Microbiology, Laboratory of Molecular of Biology, Immunology and Bioinformatics, Adeleke University, P.M.B. 250, Ede, Osun State, Nigeria*
[e] *Department of Biochemistry, Adeleke University, P.M.B. 250, Ede, Osun State, Nigeria*
[f] *Department of Chemistry, University of Ibadan, Ibadan, Oyo State, Nigeria*
[g] *Computational Chemistry Laboratory, Department of Pure and Applied Chemistry, Ladoke Akintola University of Technology, P.M.B. 4000, Ogbomoso, Oyo State, Nigeria*

## ARTICLE INFO

## ABSTRACT

In this work, ten molecular compounds were optimised using density functional theory (DFT) method via Spartan 14. The obtained descriptors were used to develop quantitative structural activities relationship (QSAR) model using Gretl and Matlab software and the similarity between predicted $IC_{50}$ and observed $IC_{50}$ was investigated. Also, docking study revealed the non-bonding interactions between the studied compounds and the receptor. The molecular interactions between the observed ligands and brain cancer protein (PDB ID: 1q7f) were investigated. Adsorption, distribution, metabolism, excretion and toxicity (ADMET) properties were also investigated.

* Corresponding author.
  *E-mail address:* abeloyebamiji@gmail.com (A.K. Oyebamiji).

## Specifications Table

| Subject | Computational Chemistry |
|---|---|
| Specific subject area | Drug Discovery and Development |
| Type of data | Figure |
| | Table |
| | QSAR model |
| How data were acquired | Spartan'14, Pymol 1.7.4.4, Autodock tool 1.5.6, AutoVina 1.1.2, Discovery Studio 2017. |
| Data format | Raw data |
| Parameters for data collection | B3LYP, 6–31G*, Pymol 1.7.4.4, Discovery studio 2017R, Autodock tool 1.5.6 and Autodock vina 1.1.2. |
| Description of data collection | The research work started with optimizing the selected compounds using DFT. The obtained descriptors from the optimized compounds were extracted and used to develop QSAR model using MLR and Genetic Algrithm. Also, the developed QSAR model was used to predict the biological activites of new set of triazole based drug-like comounds and further subjected to docking. The results obtained were collected and interpreted. |
| Data source location | Computational Chemistry Research Laboratory, Department of Pure and Applied Chemistry, Ladoke Akintola University of Technology, P.M.B. 4000, Ogbomoso, Oyo State, Nigeria. |
| Data accessibility | The observed and calculated data can be accessed with the data article |

## Value of the Data

- The data obtained from investigated triazole derivatives in this research will assist scientists to know the molecular descriptors that describe its anti-glioblastoma activity.
- Data in this research will disclose the role of individual molecular descriptors obtained from optimised compounds in the developed QSAR model.
- The obtained binding affinity will reveal the ability of each compound to inhibit brain tumor protein (PDB ID: 1q7f).
- ADMET properties of the observed and proposed molecular compounds were also investigated in order to define the nature of triazole derivatives in receptor.
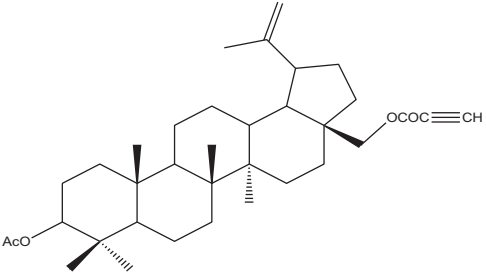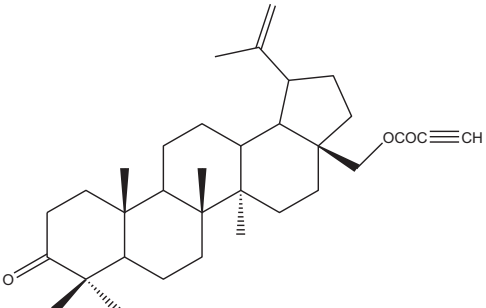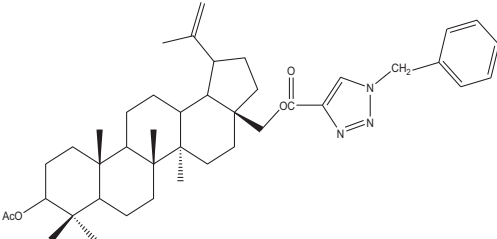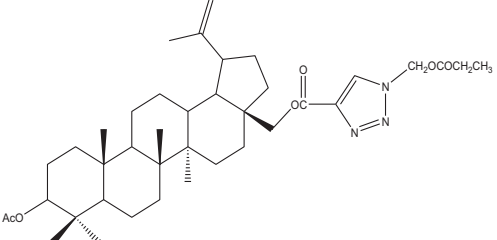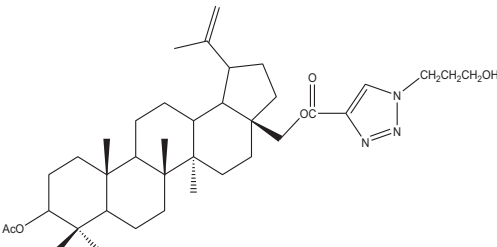
## 1. Data Description

The 2D structures of the molecules used in this research were shown in Table 1. The observed compounds used in this work were obtained from the research carried out by Ewa et al., (2018) [1]. The compounds with inhibition concentration ($IC_{50}$) of $\leq 10\,\mu M$ were selected and subjected to quantum chemical calculation using density functional theory via B3LYP (6–31G∗basis set).

Thirteen descriptors (Table 2) which describe anti-glioblastoma activities of the investigated triazole derivative were obtained and they were used for further research. The descriptors obtained were highest occupied molecular orbital energy ($E_{HOMO}$), lowest unoccupied molecular orbital ($E_{LUMO}$), band gap (BG), molecular weight (MW), area, volume, polar surface area (PSA), ovality, dipole moment (DM), log P, polarisability (POL), hydrogen bond donor (HBD) and hydrogen bond acceptor (HBA).

Table 3 revealed the developed QSAR model (which help to probe into biological activities of triazoles derivatives) from the calculated molecular descriptor obtained from

**Table 1**
The Schematic diagram of the observed Triazole derivatives [1].

| SN | Molecular Structures | IUPAC Name |
|---|---|---|
| 1 | | 3-Acetyl-28-propynoylbetulin |
| 2 | | 28-Propynoylbetulone |
| 3 | | 3-Acetyl-28-[1-(4-*fluorobenzyl*)−1H-1,2,3-*triazol-4-yl*]carbonylbetulin |
| 4 | | 3-Acetyl-28-(1-ethylacetyl-1H-1,2,3-triazol-4-yl)carbonylbetulin |
| 5 | | 3-Acetyl-28-[1-(3-*hydroxypropyl*)−1H-1,2,3-*triazol-4-yl*]carbonylbetulin |

(*continued on next page*)

**Table 1** (_continued_)

| SN | Molecular Structures | IUPAC Name |
|---|---|---|
| 6 |  | 2-Amino-3-[4-(3-_acetyl_-28-_betulinylcarbonyl_)−1H-1,2,3-_triazol_-1-_yl_]propanoic acid |
| 7 |  | 28-[1-(4-_Fluorobenzyl_)−1H-1,2,3-_triazol_-4-_yl_]carbonylbetulone |
| 8 |  | 28-[1-(4-_Cyanobenzyl_)−1H-1,2,3-_triazol_-4-_yl_]carbonylbetulone |
| 9 |  | 28-[1-(3′-_Deoxythymidine_-5′-_yl_)−1H-1,2,3-_triazol_-4-_yl_]carbonylbetulone |
| 10 |  | 28-[1-(1-D_eoxy_-β-D-_glucopyranosyl_)−1H-1,2,3-_triazol_-4-_yl_]carbonylbetulone |

**Table 2**

Calculated molecular descriptors with anti-glioblastoma activities.

|  | $E_{HOMO}$ | $E_{LUMO}$ | BG | DM | MW | AREA | VOL | PSA | OVA | LOG P | POL | HBD | HBA |
|---|---|---|---|---|---|---|---|---|---|---|---|---|---|
| 1 | −6.30 | **−2.75** | **3.55** | 3.72 | 536.79 | 571.38 | 598.14 | 40.09 | 1.66 | 8.09 | 89.06 | 0 | 2 |
| 2 | −6.29 | −1.49 | 4.80 | 3.76 | 492.74 | 521.02 | 551.1 | 33.37 | 1.60 | 8.35 | 84.95 | 0 | 2 |
| 3 | −6.36 | −0.99 | 5.37 | 6.72 | 673.95 | 706.89 | 726.39 | 51.01 | 1.81 | 10.23 | 99.03 | 0 | 5 |
| 4 | −6.33 | −1.00 | 5.33 | 7.57 | 651.93 | 692.8 | 704.58 | 71.86 | 1.81 | 8.21 | 97.27 | 0 | 6 |
| 5 | −6.39 | −0.96 | 5.43 | 7.58 | 623.92 | 668.32 | 681.66 | 71.04 | 1.78 | 8.10 | 95.39 | 1 | 6 |
| 6 | −6.36 | −1.02 | 5.34 | 6.29 | 652.92 | 682.91 | 695.04 | 109.53 | 1.80 | 6.86 | 96.49 | 1 | 7 |
| 7 | −6.25 | −1.04 | 5.21 | 5.98 | 643.88 | 659.42 | 682.81 | 59.30 | 1.76 | 10.02 | 95.53 | 0 | 5 |
| 8 | −6.28 | −1.92 | 4.36 | 4.46 | 650.90 | 674.84 | 697.86 | 74.64 | 1.77 | 9.90 | 96.95 | 0 | 6 |
| 9 | −6.28 | −1.12 | 5.16 | 6.23 | 759.98 | 760.65 | 777.32 | 125.34 | 1.86 | 7.12 | 103.21 | 2 | 11 |
| 10 | −6.26 | −1.15 | 5.11 | 4.81 | 697.91 | 692.16 | 711.58 | 138.97 | 1.80 | 6.03 | 97.89 | 4 | 10 |

**Table 3**

Calculated QSAR model for the observed triazole derivatives.

| Equation | F | P-value | $R^2$ | Adjusted $R^2$ | MSE |
|---|---|---|---|---|---|
| $IC_{50} = -88,509.7 - 513.940(E_{HOMO}) + 500.156(E_{LUMO}) - 174.603(VOL) + 11.3407(Log\ P) + 2137.77(POL) + 0.587370(PSA) + 1.01540(AREA)$ | 31.03 | $P < 0.0001$ | 0.990 | 0.958 | 0.085 |

**Table 4**

Assessment for validation of Developed QSAR model.

| QSAR model validation parameters | Standard value | Developed QSAR model value | Remark |
|---|---|---|---|
| Correlation coefficient ($R^2$) | $\geq 0.5$ | 0.990 | Pass |
| Adjusted Correlation coefficient | $\geq 0.6$ | 0.958 | Pass |
| Confidence interval at 95% confidence level i.e. P-value | $< 0.05$ | 0.031 | Pass |

**Table 5**

Observed $IC_{50}$ and predicted $IC_{50}$.

|  | Observed $IC_{50}$ | Predicted $IC_{50}$ | Residual | Genetic Algorithm (GA) | Residual |
|---|---|---|---|---|---|
| 1 | 0.67 | 0.45 | 0.217310 | 0.616731 | 0.053269 |
| 2 | 0.19 | 0.49 | −0.307571 | 0.136731 | 0.053269 |
| 3 | 0.85 | 0.50 | 0.342669 | 0.816023 | 0.033977 |
| 4 | 0.78 | 0.74 | 0.0302183 | 0.746023 | 0.033977 |
| 5 | 7.75 | 7.91 | −0.161626 | 7.716023 | 0.033977 |
| 6 | 1.22 | 1.19 | 0.0226067 | 1.186023 | 0.033977 |
| 7 | 0.45 | 0.28 | 0.167543 | 0.416023 | 0.033977 |
| 8 | 6.45 | 6.72 | −0.270293 | 6.416796 | 0.033204 |
| 9 | 0.17 | 0.67 | −0.500773 | 0.137068 | 0.032932 |
| 10 | 7.45 | 6.99 | 0.459915 | 7.417068 | 0.032932 |

optimised compounds using Gretl software and Matlab [2,3]. The selected descriptors used in developing QSAR model were $E_{HOMO}$, $E_{LUMO}$, Vol, Log P, Pol, PSA and Area and the statistical factors considered for QSAR validation were correlation coefficient ($R^2$), adjusted correlation coefficient (Adj.$R^2$), P-Value, F-Value and MSE. The calculated value for correlation coefficient ($R^2$), Adjusted correlation coefficient (Adj. $R^2$), P-Value and F-Value were 0.990, 0.958, $P < 0.0001$, 31.03 and 0.085 as shown in Table 4.

Table 5 showed the calculated inhibition concentration ($IC_{50}$) for the investigated molecular compounds. The correlation between the predicted inhibition efficiency ($IC_{50}$) and observed efficiency ($IC_{50}$) were displayed in Fig. 1. In this work, six (6) molecular compounds were proposed using the developed QSAR model and the inhibition concentration of individual proposed compound was predicted and displayed in Table 6.
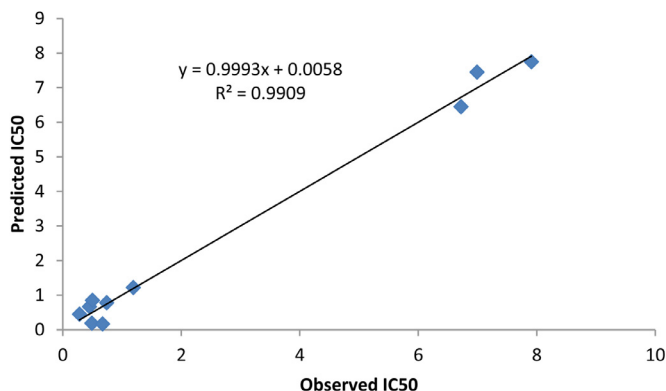
**Fig. 1.** Graphical description of correlation between predicted $IC_{50}$ and Observed $IC_{50}$.

**Table 6**
Schematics structures of the proposed compounds with the inhibition concentration.



| | $R_1$ | $R_2$ | $IC_{50}$ |
|---|---|---|---|
| 1 | $OCH_3$ | $CH_3$ | −13.54 |
| 2 | $OC_2H_5$ | $CH_3$ | −9.60 |
| 3 | $NH_2$ | $CH_3$ | −16.79 |
| 4 | $CH_3$ | $CH_3$ | −7.72 |
| 5 | $CH_2F$ | $CH_3$ | −27.30 |
| 6 | $CHF_2$ | $CH_3$ | −32.98 |

Also, Table 7 showed four molecular compounds (**2, 7, 9** and **10**) with −9.5 kcal/mol, −11.2 kcal/mol, −10.0 kcal/mol, and −9.4 kcal/mol respectively. The selected compounds were subjected to ADMET study using admetSAR server and the factor considered were based on adsorption, distribution, metabolism, excretion and toxicity of the investigated ligands. The obtained ADMET values were compared to the standard compound used (Carmustine).

The calculated molecular interaction observed between the optimised triazole derivatives and brain tumor protein (PDB ID: 1q7f) [4] were reported in Table 8. The binding affinity calculated for each complex was −8.4 kcal/mol, −9.5 kcal/mol, −8.6 kcal/mol, −8.8 kcal/mol, −8.5 kcal/mol, −8.1 kcal/mol, −11.2 kcal/mol, −9.0 kcal/mol, −10.0 kcal/mol and −9.4 kcal/mol for compound **1–10** and the interaction between the observed complexes were shown in Fig. 2.

## 2. Design, Materials and Methods

The studied triazole derivatives (Table 1) were drawn using ChemDraw Ultra 8.0 and were optimised using Spartan 14 [5]. The optimization was accomplished using B3LYP with 6–31 G*

**Table 7**
Obtained calculated ADMET Properties.

| Mode | Compound 2 Result | Compound 2 Probability | Compound 7 Result | Compound 7 Probability | Compound 8 Result | Compound 8 Probability | Compound 9 Result | Compound 9 Probability | Compound 10 Result | Compound 10 Probability | Carmustine Result | Carmustine Probability |
|---|---|---|---|---|---|---|---|---|---|---|---|---|
| Blood-Brain Barrier | BBB+ | 0.9079 | BBB+ | 0.5892 | BBB+ | 0.5456 | BBB- | 0.8875 | BBB- | 0.9564 | BBB+ | 0.9533 |
| Human Intestinal Absorption | HIA+ | 0.9900 | HIA+ | 0.9962 | HIA+ | 0.9947 | HIA+ | 0.9430 | HIA+ | 0.6024 | HIA+ | 1.0000 |
| Caco-2 Permeability | Caco2+ | 0.6469 | Caco2- | 0.5649 | Caco2- | 0.5831 | Caco2- | 0.6729 | Caco2- | 0.6997 | Caco2- | 0.5621 |
| P-glycoprotein Substrate | Substrate | 0.6290 | Substrate | 0.8512 | Substrate | 0.8125 | Substrate | 0.8454 | Substrate | 0.8269 | Non-Substrate | 0.7552 |
| P-glycoprotein Inhibitor | Inhibitor | 0.9030 | Inhibitor | 0.9365 | Inhibitor | 0.9495 | Inhibitor | 0.6937 | Inhibitor | 0.7651 | Non-inhibitor | 0.7970 |
| Renal Organic Cation Transporter | Non-inhibitor | 0.7387 | Non-inhibitor | 0.5700 | Non-inhibitor | 0.5301 | Non-inhibitor | 0.8682 | Non-inhibitor | 0.9224 | Non-inhibitor | 0.8177 |
| Subcellular localization | Mitochondria | 0.8457 | Mitochondria | 0.6253 | Mitochondria | 0.6304 | Mitochondria | 0.5907 | Mitochondria | 0.4545 | Mitochondria | 0.7342 |
| CYP450 2C9 Substrate | Non-substrate | 0.8652 | Non-substrate | 0.8442 | Non-substrate | 0.8067 | Non-substrate | 0.7938 | Non-substrate | 0.7848 | Non-substrate | 0.7656 |
| CYP450 2D6 Substrate | Non-substrate | 0.9104 | Non-substrate | 0.8250 | Non-substrate | 0.8210 | Non-substrate | 0.8343 | Non-substrate | 0.8260 | Non-substrate | 0.8491 |
| CYP450 3A4 Substrate | Substrate | 0.7739 | Substrate | 0.6987 | Substrate | 0.7062 | Substrate | 0.7076 | Substrate | 0.6901 | Non-substrate | 0.6720 |
| CYP450 1A2 Inhibitor | Non-inhibitor | 0.8848 | Non-inhibitor | 0.7102 | Non-inhibitor | 0.7503 | Non-inhibitor | 0.8277 | Non-inhibitor | 0.7723 | Non-inhibitor | 0.9045 |
| CYP450 2C9 Inhibitor | Non-inhibitor | 0.6679 | Non-inhibitor | 0.5957 | Non-inhibitor | 0.6198 | Non-inhibitor | 0.6658 | Non-inhibitor | 0.7210 | Non-inhibitor | 0.9070 |
| CYP450 2D6 Inhibitor | Non-inhibitor | 0.9248 | Non-inhibitor | 0.8454 | Non-inhibitor | 0.8666 | Non-inhibitor | 0.8863 | Non-inhibitor | 0.9026 | Non-inhibitor | 0.9231 |
| CYP450 2C19 Inhibitor | Inhibitor | 0.5296 | Inhibitor | 0.5581 | Non-inhibitor | 0.5391 | Non-inhibitor | 0.7017 | Non-inhibitor | 0.7290 | Non-inhibitor | 0.9025 |
| CYP450 3A4 Inhibitor | Non-inhibitor | 0.6446 | Non-inhibitor | 0.7561 | Inhibitor | 0.7227 | Inhibitor | 0.9283 | Inhibitor | 0.6378 | Non-inhibitor | 0.9031 |
| CYP Inhibitory Promiscuity | Low CYP Inhibitory Promiscuity | 0.5796 | High CYP Inhibitory Promiscuity | 0.8442 | High CYP Inhibitory Promiscuity | 0.7893 | High CYP Inhibitory Promiscuity | 0.6255 | High CYP Inhibitory Promiscuity | 0.5093 | Low CYP Inhibitory Promiscuity | 0.9131 |
| Human Ether-a-go-go-Related Gene Inhibition | Weak inhibitor | 0.9102 | Weak inhibitor | 0.6081 | Weak inhibitor | 0.5223 | Weak inhibitor | 0.7555 | Weak inhibitor | 0.9532 | Strong inhibitor | 0.7278 |
| | Non-inhibitor | 0.7874 | Non-inhibitor | 0.5632 | Non-inhibitor | 0.7159 | Non-inhibitor | 0.7011 | Non-inhibitor | 0.5634 | Non-inhibitor | 0.9190 |
| AMES Toxicity | Non AMES toxic | 0.8923 | Non AMES toxic | 0.5299 | Non AMES toxic | 0.5228 | Non AMES toxic | 0.5140 | Non AMES toxic | 0.5885 | AMES toxic | 0.9577 |
| Carcinogens | Non-carcinogens | 0.8769 | Non-carcinogens | 0.8221 | Non-carcinogens | 0.8539 | Non-carcinogens | 0.7862 | Non-carcinogens | 0.9015 | Carcinogens | 0.6880 |
| Fish Toxicity | High FHMT | 0.9996 | High FHMT | 1.0000 | High FHMT | 0.9999 | High FHMT | 0.9998 | High FHMT | 0.9999 | High FHMT | 0.6546 |
| Tetrahymena Pyriformis Toxicity | High TPT | 0.9996 | High TPT | 0.9968 | High TPT | 0.9931 | High TPT | 0.9874 | High TPT | 0.9924 | High TPT | 0.9857 |
| Honey Bee Toxicity | High HBT | 0.8781 | Low HBT | 0.6610 | Low HBT | 0.5742 | Low HBT | 0.6662 | Low HBT | 0.6038 | Low HBT | 0.7045 |
| Biodegradation | Not ready biodegradable | 0.9800 | Not ready biodegradable | 1.0000 | Not ready biodegradable | 1.0000 | Not ready biodegradable | 0.9870 | Not ready biodegradable | 0.9803 | Not ready biodegradable | 0.5596 |

**Table 8**
Scoring and residues involved in the interaction between the studied complex.

| | Scoring (kcal/mol) | Residues involved in the interactions | Types of Non-bonding interaction involved |
|---|---|---|---|
| **1** | −8.4 | VAL-835, VAL-788, VAL-921, LEU-1sss009, ILE-965 | Conventional Hydrogen Bond, Alkyl |
| **2** | −9.5 | GLY-964, VAL-921, ALA-787, ARG-837, ILE-965 | Carbon Hydrogen Bond, Alkyl |
| **3** | −8.6 | ILE-965, VAL-1007, ALA-787, ALA-834, VAL-922, ARG-837 | Carbon Hydrogen Bond, Alkyl |
| **4** | −8.8 | ASP-924, ARG-837, ALA-834, VAL-877 | Conventional Hydrogen Bond, Carbon Hydrogen Bond, Pi-Alkyl, Alkyl |
| **5** | −8.5 | ASP-924, ILE-965, VAL-950, THR-878, LEU-1009, ALA-1008, ARG-837 | Conventional Hydrogen Bond, Carbon Hydrogen Bond, Pi-Alkyl, Alkyl |
| **6** | −8.1 | THR-986, GLN-987, GLY-969, ASN-968, ILE-965, VAL-922, ARG-837, VAL-835 | Conventional Hydrogen Bond, Carbon Hydrogen Bond, Alkyl |
| **7** | **−11.2** | ARG-837, ALA-1008, ASP-1006, VAL-877, VAL-833, LEU-1009, ILE-965 | Conventional Hydrogen Bond, Halogen(Fluorine), Pi-Anion, Pi-Alkyl, Alkyl |
| **8** | −9.0 | ILE-965, GLY-969, VAL-922, ARG-837, ALA-1008, ALA-787 | Carbon Hydrogen Bond, Alkyl |
| **9** | −10.0 | ILE-965, ALA-787, ALA-834, VAL-922, ARG-837, ALA-790 | Conventional Hydrogen Bond, Carbon Hydrogen Bond, Pi-Alkyl, Pi-Sigma, Alkyl |
| **10** | −9.4 | ILE-965, ALA-787, ALA-1008, VAL-922, ASN-838, ARG-837 | Conventional Hydrogen Bond, Carbon Hydrogen Bond, Pi-Alkyl, Alkyl |
| **Carmustine** | −5.0 | VAL-835, ARG-837, VAL-879 | Conventional Hydrogen Bond |
| **Proposed Compounds** | | | |
| **P1** | −8.6 | PHE-916, ILE-961, TYR-959 | Alkyl, Pi-Alkyl |
| **P2** | −8.7 | PHE-916, ILE-961, TYR-959 | Alkyl, Pi-Alkyl |
| **P3** | −8.5 | VAL-788, VAL-835, ARG-837, ILE-965 | Conventional Hydrogen Bond, Unfavourable Donor-Donor, Alkyl |
| **P4** | −8.7 | PHE-916, ILE-961, TYR-959 | Alkyl, Pi-Alkyl |
| **P5** | −8.6 | PHE-1005, PHE-916, ILE-961, TYR-959 | Alkyl, Pi-Alkyl |
| **P6** | −8.9 | ARG-837, VAL-788, ALA-787, VAL-835, ALA-834, ILE-965, VAL-921 | Conventional Hydrogen Bond, Halogen, Alkyl |

as basis set which produce descriptors that were used for further investigation. The selected calculated descriptors obtained from the optimised compounds were used to build robust QSAR model in order to relate the biological activity of the studied compounds to the calculated molecular parameters [6]. This was achieved using mathematical methods (multiple linear regression method) via Gretl 1.9.8. The observed inhibition concentration ($IC_{50}$) served as dependent variable while the calculated descriptors served as independent variables; thus, the QSAR model was developed. Several factors such as correlation coefficient ($R^2$), P-Value, F-value were considered to know the level of efficiency of the developed QSAR model. More so, validation of the developed QSAR model was implemented by observing some mathematical factors (cross validation correlation coefficient (C.V $R^2$), adjusted correlation coefficient) which could be calculated using Eq. (1) and 2 [7].

$$C.VR^2 = 1 - \frac{\sum (Y_{obs} - Y_{cal})^2}{\sum (Y_{obs} - \bar{Y}_{obs})^2} \tag{1}$$

$$R_a^2 = \frac{(N-1) \times R^2 - P}{N - 1 - P} \tag{2}$$

Absorption, Distribution, Metabolism, Excretion and the Toxicity properties of the studied triazole derivatives were done via online software (admetSAR) (http://lmmd.ecust.edu.cn/admetsar1) [8]. The factors considered were Blood Brain Barrier, Caco-2 cell permeability, Human Intestinal Absorption, Ames test. Also, four software (Pymol
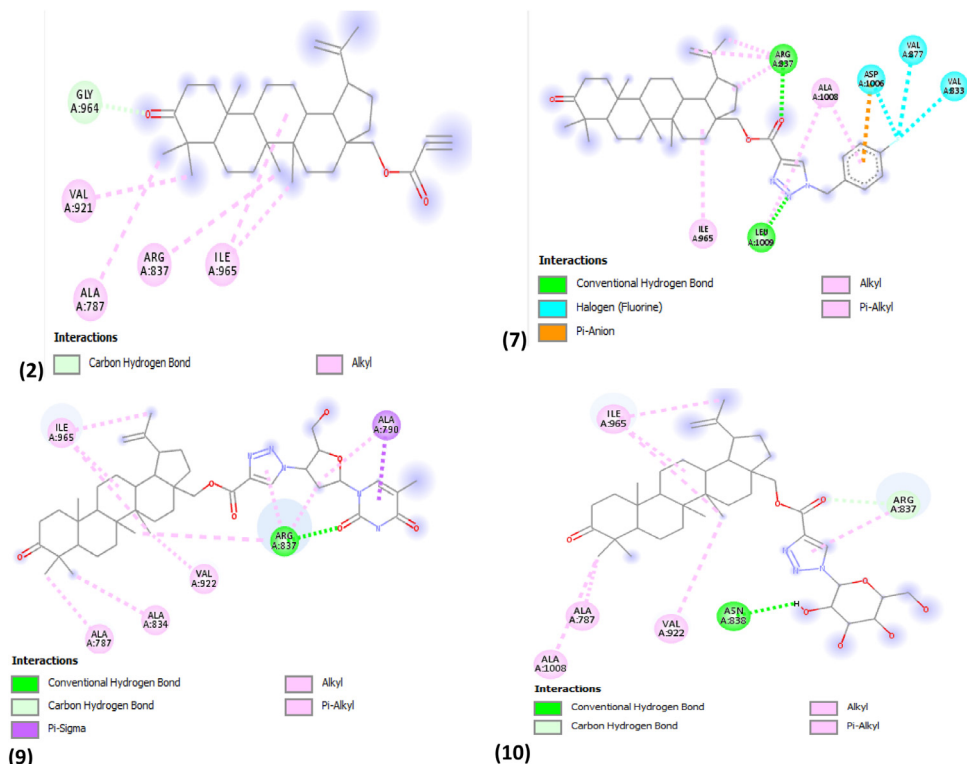
**Fig. 2.** 2D structures of brain tumor protein (PDB ID: 1q7f) and compound **2, 7, 8, 9** and **10** respectively.

(for treating downloaded protein), Autodock Tool (for locating binding site in the downloaded protein and for converting ligand and receptor to.pdbqt format from.pdb format), Auto dock vina (for docking calculation) and discovery studio (for viewing the non-bonding interaction between the docked complexes) were used to accomplish docking study between triazole derivative and brain tumor protein (PDB ID: 1q7f). The observed grid box was as follows: center ($X = 12.534$, $Y = 23.847$, $Z = 40.848$) and size ($X = 68$, $Y = 64$, $Z = 72$) as well as the spacing was set to be $1.00 \, \text{Å}$.

## Ethics Statement

Not Applicable.

## CRediT Author Statement

Abel Kolawole **OYEBAMIJI:** Conceptualization, Methodology, Writing- Original draft preparation; Oluwatumininu Abosede **MUTIU**: Software; Folake Ayobami **AMAO**, Data curation; Olubukola Monisola **OYAWOYE**: Writing- Reviewing and Editing; Temitope A **OYEDEPO:** Writing-Reviewing and Editing; Babatunde Benjamin **ADELEKE**: Visualization; Banjo **SEMIRE:** Supervision, Software, Validation.

## Declaration of Competing Interest

The authors declare that they have no conflict of interest.

## Acknowledgement

## References

[1] B. Ewa, K.-.T. Monika, C. Elwira, L. Małgorzata, B. Stanisław, Novel triazoles of 3-acetylbetulin and betulone as anticancer agents, Med. Chem. Res. 27 (2018) 2051–2061.

[2] A.Beheshti, E.Pourbasheer, M. Nekoei, S. Vahdani, QSAR modeling of antimalarial activity of urea derivatives using genetic algorithm–multiple linear regressions, J. Saudi Chem. Soc., (2012), 10.1016/j.jscs.2012.07.019

[3] A. Ousaa, B. Elidrissi1, M. Ghamali, S. Chtita, A. Aouidate, M. Bouachrine, T. Lakhlifi, Quantitative structure-toxicity relationship studies of aromatic aldehydes to Tetrahymena pyriformis based on electronic and topological descriptors, J. Mater. Environ. Sci. 9 (1) (2018) 256–266.

[4] A.E. Thomas, B.D. Wilkinson, R.P. Wharton, A.K. Aggarwal, Model of the brain tumor–pumilio translation repressor complex, Genes Dev. 17 (2015) 2508–2513.

[5] Spartan 14 program, Wavefunction, Irvine, USA.

[6] A.K. Oyebamiji, I.O. Abdulsalami, B. Semire, Dataset on Insilico approaches for 3,4-dihydropyrimidin-2(1H)-one urea derivatives as efficient Staphylococcus aureus inhibitor, Data Brief 32 (2020) 106195.

[7] R.O. Oyewole, A.K. Oyebamiji, B. Semire, Theoretical calculations of molecular descriptors for anticancer activities of 1, 2,3-triazole-pyrimidine derivatives against gastric cancer cell line (MGC-803): DFT, QSAR and docking approaches, Heliyon 6 (2020) e03926.

[8] S. Jie, C. Feixiong, X. You, L. Weihua, T. Yun, Estimation of ADME properties with substructure pattern recognition, J. Chem. Inf. Model. 50 (2010) 1034–1041.